HHS Public Access

Author manuscript

Free Radic Biol Med. Author manuscript; available in PMC 2023 March 23.

Published in final edited form as:

Free Radic Biol Med. 2020 February 01; 147: 48–60. doi:10.1016/j.freeradbiomed.2019.12.018.

Scavenging reactive oxygen species selectively inhibits M2 macrophage polarization and their pro-tumorigenic function in part, via Stat3 suppression

Brandon Griess[1], **Shakeel Mir**[1], **Kaustubh Datta**[1], **Melissa Teoh-Fitzgerald**[1]

[1]Department of Biochemistry and Molecular Biology, Fred and Pamela Buffett Cancer Center, College of Medicine, University of Nebraska Medical Center, Omaha, NE 68198, USA

Abstract

Tumor associated macrophages (TAM) enhance the aggressiveness of breast cancer via promoting cancer cell growth, metastasis, and suppression of the patient's immune system. These TAMs are polarized in breast cancer with features more closely resembling the pro-tumorigenic and immunosuppressive M2 type rather than the anti-tumor and pro-inflammatory M1 type. The goal of our study was to examine primary human monocyte-derived M1 and M2 macrophages for key redox differences and determine sensitivities of these macrophages to the redox-active drug, MnTE-2-PyP^{5+}. This compound reduced levels of M2 markers and inhibited their ability to promote cancer cell growth and suppress T cell activation. The surface levels of the T cell suppressing molecule, PD-L2, were reduced by MnTE-2-PyP^{5+} in a dose-dependent manner. This study also examined key differences in ROS generation and scavenging between M1 and M2 macrophages. Our results indicate that M2 macrophages have lower levels of reactive oxygen species (ROS) and lower production of extracellular hydrogen peroxide compared to the M1 macrophages. These differences are due in part to reduced expression levels of pro-oxidants, Nox2, Nox5, and the non-enzymatic members of the Nox complex, p22phox and p47phox, as well as higher levels of antioxidant enzymes, Cu/ZnSOD, Gpx1, and catalase. More importantly, we found that despite having lower ROS levels, M2 macrophages require ROS for proper polarization, as addition of hydrogen peroxide increased M2 markers. These TAM-like macrophages are also more sensitive to the ROS modulator and a pan-Nox inhibitor. Both MnTE-2-PyP^{5+} and DPI inhibited expression levels of M2 marker genes. We have further shown that this inhibition was partly mediated through a decrease in Stat3 activation during IL4-induced M2 polarization. Overall, this study reveals key redox differences between M1 and M2 primary human macrophages and that redox-active drugs can be used to inhibit the pro-tumor and immunosuppressive phenotype of TAM-like M2 macrophages. This study also provides rationale for combining MnTE-2-PyP^{5+} with immunotherapies.

Keywords

Tumor Associated Macrophages; Stat3; SOD mimetics; ROS; Immunosuppression; Breast Cancer

Corresponding Author: Melissa Teoh-Fitzgerald, 7005 Durham Research Center, 985870 Nebraska Medical Center, Omaha, NE 68198-5870, Tel: (402) 559-7072, Fax: (402) 559-6650, m.teohfitzgerald@unmc.edu.

The authors declare no conflict

1. Introduction:

Macrophages are known to exhibit high plasticity which allows for dramatically different functions based on signals received from the microenvironment. In general, macrophages can polarize toward two extremes, the proinflammatory M1 and the immunosuppressive M2. The classically activated M1 macrophages are characterized by enhanced bacteria killing via an oxidative burst of reactive oxygen species (ROS), increased antigen presentation and phagocytosis, high IL-12 production, and promotion of a T_H1 response. Conversely, M2 macrophage are characterized by increased efferocytosis, high IL-10 secretion, high levels of scavenger receptors, such as CD163 and CD206, promotion of a T_H2 response, and immunosuppression. This is, however, an oversimplification of the complexity of macrophage polarization as recent studies indicate a much broader range of polarization states, such M2b, M2c, Mox, and M4, depending on the stimulating factor(s) within the milieu, as detailed in the these reviews [1, 2].

Macrophages are the most abundant immune cell in the tumor stroma and can account for up to 50% of tumor mass in breast cancer [3]. These tumor-associated macrophages (TAMs) are known to promote cancer cell growth, metastasis, and cancer cell evasion of the immune system [4]. Then unsurprisingly, TAMs are correlated with decreased survival in many types of solid cancers, such as breast, lung, and pancreatic, among others [5–15]. While TAM are a heterogeneous population, they are mostly skewed toward a predominantly M2 phenotype [16]. The M2 surface marker, CD163, is correlated with poor patient survival, metastasis, and grade in breast cancer [17–20]. Macrophage depletion in mouse models decreases tumor growth and metastasis [21–23]. Therefore, a further understanding of the M2 macrophages polarization and function is required to develop therapies to target their detrimental effects seen in many different solid cancers.

During activation, M1 macrophages produce ROS via Nox2 to activate NF-κB, thereby stimulating phagocytosis and the inflammasome [24]. However, few studies have investigated the role of ROS in M2 polarization and function. Some studies suggest that M2 macrophages have key differences in ROS production and metabolism compared to M1 macrophages [24]. Promoting a pro-oxidative condition by lowering glutathione (GSH) levels has been shown to increase IL-10 and decreased IL-12 production in macrophages, indicative of a more M2 polarization state [25]. Conversely, increasing glutathione levels promoted M1 polarization as shown by an increase in IL-12 production and a decrease in IL-10 levels [25]. Therefore, the redox status of macrophages could be a contributing factor of macrophage polarization and function. Furthermore, butylated hydroxyanisole (BHA), a commonly used food preservative that prevents fatty acid oxidation, inhibits M-CSF mediated M2 polarization [26]. However, BHA also has off-target effects, such as disruption of the electron transport chain, which could also disrupt macrophage polarization [27]. Despite all the recent advancements in understanding macrophage biology, the direct role of ROS during TAM or M2 polarization and function remains unclear.

MnTE-2-PyP^{5+} (MnTE), also known as AEOL10113 and BMX-010, is a member of the manganese porphyrin (MnP) ring family of redox-active drugs. MnTE has been safely

administered in preclinical models with very little negative side effects [28]. It is currently used in clinical trials for atopic dermatitis and plaque psoriasis. Additionally, an analog of MnTE, MnTnBuOE-2-PyP^{5+}, is also being tested as a radioprotectant in patients with multiple brain metastases, anal cancer, high grade glioma, and advanced head and neck cancer. MnPs were initially designed to mimic the activity of superoxide dismutases (SODs). However, the small molecule MnPs lack the large protein bulk of SODs, which provide selectivity toward $O_2^{\bullet-}$ via steric hindrance. Thus, MnPs have a more promiscuous active site that can readily react with other reactive species, such as peroxynitrite and hydrogen peroxide [29]. Furthermore, recent evidence indicates that MnPs can act as a pro-oxidant in certain cancer cell lines and in tumor tissue. This effect is especially potent when MnPs are combined with high levels of intravenous ascorbate and/or radiation [30–32]. Interestingly, there is some circumstantial evidence that MnTE may affect macrophages in breast cancer. MnTE treatment in the 4T1 mouse model of stage IV breast cancer reduced macrophage infiltration, along with reduced levels of angiogenesis and metastasis, which are both processes induced by M2 macrophages [33]. This study provided rationale for determining the effect of MnTE on macrophage polarization and function directly.

Tumors are known to have a highly oxidative microenvironment compared to adjacent normal tissue, in part due to an increased ROS production from cancer cells [34]. The role of this highly oxidative tumor microenvironment on the interactions between cancer cells and the surrounding stromal cells is not clear. Particularly, the influence of this oxidative tumor microenvironment on TAM function is not known. Due to the high plasticity of macrophages and the key role they play in the immune response to cancer, we sought to determine the role of ROS on macrophage polarization and function. The objectives here were to characterize key redox profile in pro-tumorigenic M2 macrophages versus anti-tumorigenic M1 macrophages and to determine differences in their sensitivity to MnTE, with the goal of selectively targeting the M2 macrophages. We found that M2 macrophages showed an increase expression levels of some key antioxidant enzymes and lower levels of some pro-oxidants, when compared to the M1 macrophages, suggesting an increase ability to tolerate an oxidative environment. Interestingly, despite the lower levels of ROS levels in M2 macrophages, these cells seem to require an optimum range of ROS to maintain their proper function and are more sensitive to ROS scavengers. Polarization of the M2 but not the M1 macrophages was attenuated by the redox-active drug, MnTE and the pan-Nox inhibitor, diphenyleneiodonium (DPI) [35]. These data suggest that the M1 macrophages can tolerate a wider range of ROS levels whereas the M2 macrophages are more vulnerable to alterations in cellular redox status. We have further shown that MnTE inhibited IL4-stimulated polarization of M2 macrophages by decreasing Stat3 activation. Consequently, MnTE treated macrophages showed reduced ability to promote breast cancer cell growth and T cell suppression. This study highlights a critical role of ROS in M2 macrophage function and implies that targeting the redox susceptibility of these macrophages could be a promising consideration for a more effective anti-cancer strategy.

2. Materials and Methods:

2.1. Cells/Cell lines and Growing Conditions:

Peripheral blood mononuclear cells (PBMCs) were isolated from human donor whole blood. Primary human monocytes and peripheral blood leukocytes were separated via elutriation by the UNMC Elutriation core. Monocytes and PBLs were used immediately after separation or were cryopreserved in liquid nitrogen before use. Breast cancer cell line, MDA-MB231 was obtained from ATCC. PBMCs, monocytes, leukocytes, and MDA-MB231 were maintained at 37˚C in 5% CO_2 in RPMI media with glutamine, 10% fetal bovine serum, penicillin and streptomycin added. Macrophages were treated with DPI (Sigma #D2926) dissolved in DMSO or hydrogen peroxide (Sigma #216763) diluted in sterile water.

2.2. Macrophage Differentiation and Polarization:

Polarization of macrophages was induced as described [36] with the following modifications. Primary human monocytes were plated on tissue culture treated plates/dishes at 1000 cells/mm^2 growth area in complete RPMI. Monocytes were differentiated and polarized to M1 macrophages with GM-CSF (100 ng/mL, BioLegend #572904) for 7 days to promote monocyte differentiation and growth. Then, the GM-CSF stimulated macrophages were polarized to M1 by addition of IFN-γ (20 ng/mL, BioLegend #570204) and LPS (20 ng/mL, Sigma # L6529) for 24 hours. Monocytes were differentiated and polarized to M2 macrophages with M-CSF (100 ng/mL, BioLegend #574806) for 7 days to promote monocyte differentiation and growth. Then, the M-CSF stimulated macrophages were polarized to M2 by addition of IL-4 (20 ng/mL, BioLegend #574002) for 24 hours. After 24 hours of polarization both M1 and M2 macrophages were ready for down-stream applications.

2.3. ROS Measurements:

ROS was measured using dihydroethidium (DHE) (ThermoFisher #D1168) and 2',7'-dichlorodihydrofluorescein diacetate (DCFH) (ThermoFisher #C400). Macrophages were removed from the cell culture surface via Accutase (Corning #25–058-Cl). After media was harvested, macrophages were washed with cold PBS. Macrophages were incubated at room temperature with Accutase for 30 minutes. Macrophages were released from the cell culture surface with gentle pipetting with high viability for down-stream applications. After achieving single cell suspension, M1/M2 macrophages were incubated in the dark with either dye at 10 μM for 40 minutes at 37°C in Hank's Balanced Salt Solution (HBSS). Cells were then washed with HBSS and strained to ensure single cell suspension. Fluorescence was measured via flow cytometry on a BD LSRII. For DHE, superoxide-enriched fluorescence was measured using the 405nm laser, while fluorescence induced by superoxide and non-specific ROS was measured using the 488nm laser. GSH and GSSG levels were measured using GSH/GSSG-Glo assay (Promega #V6611). Macrophages were replated in a 96 well plate before the final polarization step to ensure equal number between wells. After 24 hours of polarization, the total GSH and oxidized GSSG were measured in the macrophages according to the manufacturer's protocol. The reduced GSH and GSH/GSSG ratio were calculated from those values. Amplex Red assay (ThermoFisher #A22188) measured extracellular ROS levels. Macrophages were replated into a 24 well

plate before final polarization. After 24 hours of polarization, extracellular H_2O_2 levels were measured following the manufacturer's protocol with the noted exception of using DPBS instead of Krebs-Rinder phosphate buffer and adding the Amplex Red solution to adherent macrophages. Fluorescence was measured 4 hours after addition of the Amplex Red solution. Both GSH/GSSG-glo and Amplex Red assays were measured using a TECAN Infinite M200 Pro plate reader.

2.4. Protein and RNA Isolation from Macrophages:

Protein lysate was isolated from M1/M2 macrophages using RIPA buffer and sonication for the signaling assays. To maintain enzyme activity, protein lysate was also isolated using a non-denaturing lysis buffer from Cell Signaling (Cell Signaling #9803) using sonication. RNA was isolated using a column-based kit from ZymoResearch (Quick-RNA™ MiniPrep, ZymoResearch #R1055) following the manufacturer's protocol.

2.5. qRT-PCR:

RNA from M1/M2 macrophages was converted to cDNA via reverse transcriptase (High-Capacity cDNA Reverse Transcription Kit; ThermoFisher #4368814). qRT-PCR was performed using SYBR Green (Maxima SYBR Green/ROX qPCR Master Mix; ThermoFisher #K0221) on an ABI Prism 7000 Sequence Detection System. Gene expression was determined via the $2^{-\Delta\Delta Ct}$ method with 18S as the control gene. The primers used for each gene are listed in supplemental table 1.

2.6. Western Blot:

10 μg of protein lysate was run on a 4–20% tris-glycine gel before transferred to a PVDF membrane using iBlot Dry Blotting transfer system. Membranes were probed overnight at 4˚C with the antibodies at the listed concentration found in supplemental table 2.

2.7. GPX and SOD Activity Assay:

The activity assays were performed using in-gel assays to differentiate between different isoforms of the GPX and SOD families. The GPX and SOD activity assays were performed as previously described [38, 39]. SOD activity gel used 40 μg of lysate, while the GPX activity gel used 100 μg of lysate. Both activity assays were performed with lysate prepared using non-reducing lysis buffer to retain protein activity.

2.8. Surface Marker Analysis:

Macrophages in single cell suspension were counted and antibodies were added at a concentration of 5 μL antibody per 1×10^6 cells in FACS buffer (1% BSA in HBSS without Ca^{2+}/Mg^{2+}). Cells were incubated in antibody mix for 30 minutes at room temperature. After washing, stained cells were measured using a LSRII flow cytometer. The antibodies used are listed below. When used in combination with additional antibodies, single stain controls were used to compensate for bleed over between the fluorophores. Cells were stained with the antibodies found in supplemental table 3.

2.9. T Cell Activation Assay:

Autologous T cells were procured as peripheral blood lymphocytes from the UNMC Elutriation Core after isolation from monocytes. T cells were labeled with 7.5 μM CFSE (BD Biosciences #565082) for 15 minutes at 37˚C. After washing, T cells were plated on top of treated macrophages after washing off treatment. Activation of T cells was achieved with anti-CD3 co-stimulation (OKT3, BioLegend #317302) at 0.1 μg/mL in RPMI with 10% FBS and Pen/Strep. The non-adherent T cells were washed out of the well using DPBS and re-suspended in FACS buffer before measuring CFSE using a LSRII flow cytometer.

2.10. MDA-MB231 Growth Assay:

Conditioned media from treated and untreated macrophages was collected, spun down, and filtered. This media was stored at −80˚C until use. MDA-MB231.luc (MDA-MB231 cells stably expressing luciferase) were plated in complete RPMI media in a 96 well white walled plate at a concentration of 2,000 cells per well. Conditioned media was added to the wells to make it a final concentration of 50% conditioned media. Luciferase activity was measured on day 1, 3 and 4, to assess cell growth over time in the various conditions. Luc-Screen Extended-Glow Luciferase Reporter Gene Assay system (ThermoFisher #T1035) was used according to the manufacturer's guidelines to measure luciferase on a TECAN Infinite M200 Pro plate reader.

2.11. Statistical Analysis:

Statistical analyses were performed using GraphPad Prism 7. For some experiments, a one-way or two-way ANOVA followed by post-hoc Tukey test was used to determine statistical differences between means. Other experiments used a two-tailed paired Student's t test to determine statistical differences between groups. Statistical significance was achieved when $P < 0.05$.

3. Results

3.1. MnTE reduces expression levels of M2 markers.

To determine the role of ROS during macrophage polarization, primary human macrophages were treated with MnTE during differentiation and polarization to M1 or M2. The changes to cellular morphology were the first indications this antioxidant affected macrophage polarization. When stimulated with M-CSF and IL-4, activated M2 macrophages showed an elongated morphology as demonstrated in Figure 1A, while M1 macrophages have a more rounded spherical cell shape. MnTE treatment inhibited the elongated phenotype of M2 macrophages in a dose-dependent manner (Figure 1A). The morphology of the MnTE treated M2 macrophages resembled that of the rounded phenotype in M1 macrophages. Contrary to the M2 macrophages, MnTE treatment did not affect the overall morphology of the M1 macrophages (Figure 1A). We then analyzed M1- vs. M2- specific marker expression in these macrophages and found that MnTE indeed decreased the mRNA expression of M2 markers, IL-10 and CD163 (Figure 1B). MnTE treated M1 macrophages had increased levels of the M1 marker, TNFα, as well as a trend toward an increase in IL12b, another M1 marker (Figure 1C). To further confirm the effect of MnTE on

M2 polarization, we analyzed the surface levels of the M2 markers, CD163 and CD206. Flow cytometry analysis showed that both markers were significantly decreased in a dose-dependent manner with MnTE treatment (Figure 1D–F).

3.2. MnTE inhibits M2 macrophage function *in vitro*.

We next determined the effect of MnTE on macrophage function. It is known that M1 macrophages inhibit the growth of cancer cells, while M2 macrophages promote cancer cell growth [40, 41]. Therefore, we isolated conditioned media (c.m.) from M1 and M2 macrophages with or without MnTE pre-treatment and examined its ability to affect cancer cell growth. As expected, MDA-MB231 breast cancer cells showed a decreased proliferation in the presence of c.m. isolated from the M1 macrophages, when compared to the c.m. from the M2 macrophages and unpolarized M0 macrophages (Figure 2A). While MnTE did not affect the ability of M1 macrophages to inhibit MDA-MB231 cancer cell growth, as shown in Figure 2B, c.m. from M2 macrophages pre-treated with MnTE significantly reduced cancer cell growth (Figure 2C). Since MnTE is still in the c.m. of treated macrophages, we assessed the effect of MnTE treatment alone on cancer cell growth over 4 days. Over this short time period, MnTE alone had no direct effect on the growth of breast cancer cells (Figure 2D). These data suggests that the growth inhibition of MnTE-treated M2 macrophages was due to changes to the macrophages not the effect of the drug alone. Thus, MnTE inhibits the M2 pro-tumor phenotype *in vitro*.

3.3. MnTE inhibits M2-mediated T cell suppression

Next, we examined whether MnTE pre-treatment will affect the T cell suppressive function of the M2 macrophages. To do so, we utilized autologous T cells labeled with the fluorescent dye, CFSE, to track proliferation as a marker of T cell activation. The T cells were first stimulated with anti-CD3 to promote their activation. Then, macrophages were co-cultured with T cells where they provide the secondary signal that can promote or suppress T cell activation. M2 macrophages are known to suppress T cell activation in this method [42]. In figure 3A, a representative histogram indicates the activated T cell population as a leftward shift away from the unstimulated mono-cultured T cells. The histogram also shows that stimulated T cells co-cultured with M1 macrophages have more activated T cells than those co-cultured with M2 macrophages, as indicated by the higher peaks within the activated T cell bracket. The bar graph in figure 3B shows the results of four replicates from a representative donor. This experiment was repeated with similar results in two additional donors. As expected, anti-CD3 alone in the mono-culture condition (mono) did not readily activate the T cells, while M1 macrophages activated T cells much better than their M2 counterparts. Furthermore, MnTE treatment, while having no effect on M1-stimulated T cell activation, dramatically reverted the T cell suppressive effect of the M2 macrophages (Figure 3B–C). MnTE pre-treated M2 macrophages are now able to induce T cell proliferation to the same extent as the M1 macrophages.

To determine the mechanism behind this dramatic change, we analyzed some key co-activators and co-inhibitory molecules expressed by macrophages that are known to promote/inhibit T cell activation. Amongst these are the co-activators CD80 and CD86 [43], which we found to be significantly lower in M2 macrophages compared to M1

macrophages (Figure 3D–E). MnTE treatment had no effect on CD80 or CD86 levels in M1 or M2 macrophages suggesting neither CD80 nor CD86 plays a role in the dramatic change of treated M2 macrophages promoting T cell activation. We next evaluated PD-L2, a co-inhibitory molecule expressed on M2 macrophages that is known to play a key role in M2-mediated inhibition of T cell proliferation [44]. MnTE treatment significantly decreased surface levels of PD-L2 in a dose-dependent manner (Figure 3F). This suggests that MnTE treatment inhibits M2-mediated immunosuppression in part through reduction in PD-L2 surface levels.

3.4. M2 macrophages have differential redox status compared to M1 macrophages.

Our data suggests that M2 macrophages are more sensitive to ROS manipulation than M1. Therefore, we hypothesized that inherent differences in the redox status of M1 and M2 macrophages could explain the differential effect of ROS manipulation. To determine if there were any potential redox differences in these macrophages, we analyzed the ROS levels of fully polarized M1 and M2 macrophages. M2 macrophages showed significantly lower levels of ROS as assessed by DCFH staining (Figure 4A). Additionally, DHE labeling of the superoxide-enriched fluorescence (Ex. 405nm) and the non-specific ROS fluorescence (Ex. 488nm) were both trending lower in M2 macrophages compared to M1 (Figure 4B). To further assess the overall redox status of the cells, we analyzed the levels of cellular glutathione (GSH). In general, cells that exhibit a higher level of ROS will show a higher level of oxidized GSH (GSSG). However, Figure 4C shows no significant difference in GSSG levels between the M1 and M2 macrophages while the total levels of GSH are significantly increased in M1 versus M2 macrophages (Figure 4D). This suggests that M1 macrophages maintain a higher intracellular level of GSH to combat the increased ROS seen in these classically activated macrophages, whereas the M2 macrophages are less reliant on the GSH pathway. Next, we sought to determine if the cellular ROS differences were driven by certain cellular compartments, such as an extracellular oxidative burst or an internal spike in mitochondrial ROS production. Figure 4E shows that M2 macrophages had significantly reduced extracellular hydrogen peroxide production compared to M1 macrophages. While, mitochondrial ROS levels were unchanged between M1 and M2 macrophages (Figure 4F), despite a slight decrease in mitochondrial content in M2 macrophages (Figure 4E).

3.5. M2 macrophages have reduced ROS producing enzymes.

We next determined the sources of increased ROS levels in the M2 macrophages. Due to the large disparity in extracellular hydrogen peroxide levels, we analyzed the membrane bound ROS producing enzymes, NADPH oxidases (Nox). We found that mRNA expression of Nox2, Nox5, and CYBA (p22phox) was significantly lower in M2 macrophage compared to M1 (Figure 5A). Interestingly, Duox1 and its activator DuoxA1 both were dramatically increased in M2 whereas essentially no expression of these genes was detected in M1 macrophages (Supplemental Figure 1A). Despite the dramatic increase in Duox1, Nox2 is still the most expressed Nox family member in both M1 and M2 macrophages (Ct values for real time-PCR analysis were 19 for Nox2 and 26 for Duox1 in M2 macrophages). Additionally, both M1 and M2 macrophages expressed comparably low levels of Nox1 and Nox4 (Supplemental Figure 1B). Western blot analysis showed a slight trend of decreased Nox2 expression in M2 macrophages versus donor matched M1 macrophages (Figure 5B–

C). The cytosolic subunit of Nox2 required for its activation and ROS production, p47phox, is also dramatically reduced in M2 macrophages (Figure 5B–C), suggesting that Nox2 activity is greatly reduced in these macrophages. These data may explain the dramatic differences in extracellular hydrogen peroxide production seen in Figure 4E.

3.6. M2 macrophages have differential expression of ROS scavenging enzymes.

In a further effort to determine the cause of the lower ROS levels in M2 macrophages, we examined several key antioxidant enzymes. Gene expression of both the superoxide scavenger, copper-zinc superoxide dismutase (Cu/ZnSOD), and hydrogen peroxide scavenging enzymes, glutathione peroxidase 1 (Gpx1), Gpx4, and catalase, was found to be increased in M2 macrophages (Figure 6A). The only antioxidant gene found to be increased in M1 macrophages was MnSOD (Figure 6A). However, contrary to the mRNA expression, there was no change in MnSOD protein levels and a slight increase in activity between M1 and M2 macrophages (Figure 6B–E). We found a trend toward increase in Cu/ZnSOD protein expression and activity in M2 macrophages. Additionally, M2 macrophages had higher levels of the hydrogen peroxide scavenging proteins, Gpx1 and Gpx activity, with a trend toward increased Gpx4 protein levels (Figure 6B–E).

3.7. ROS promotes IL-4 stimulated M2 polarization.

Next, we sought to determine the mechanism by which MnTE inhibits M2 polarization and function. Since MnTE is a redox-active drug, it can act as a pro-oxidant activating additional signaling pathways or an antioxidant reducing M2 signaling cascades. To determine how MnTE is acting in macrophages, both intracellular and extracellular ROS levels were measured in treated and control macrophages. Interestingly, intracellular ROS levels were unchanged in MnTE treated M1 macrophages compared to control (Figure 7A). However, MnTE significantly reduced ROS levels by almost 40% in M2 macrophages compared to control. Extracellular hydrogen peroxide levels were also reduced by 40% in MnTE-treated M2 macrophages compared to PBS control with no changes in M1 macrophages (Figure 7B). Thus, MnTE is functioning as an antioxidant during M2 polarization. To further test the role of ROS during M2 polarization, Nox-derived ROS production was inhibited using DPI. DPI reduced M2 markers similar to MnTE (Figure 7C). Additionally, directly adding exogenous hydrogen peroxide as a bolus injection during M2 polarization increased M2 markers (Figure 7D). However, the negative effects of high levels of hydrogen peroxide are seen as M2 markers begin to drop around 20 μM.

Next, MnTE was added during different times throughout M2 polarization to test if MnTE was inhibiting IL-4 signaling during M2 polarization or activating other signaling pathways such as NF-κB and Nrf2 on its own that would shift macrophage polarization toward a more M1-like state. As indicated in Figure 7E, MnTE was added throughout differentiation and polarization, just prior to polarization, half-way through polarization, and just before RNA isolation. M2 mRNA markers were measured 48 hours after IL-4 addition. Figure 7F indicates pre-treatment is required for MnTE inhibition of M2 markers. Additionally, MnTE may affect M-CSF signaling since the effect of MnTE added just before polarization was not quite as strong as the effect of MnTE treatment throughout differentiation and polarization. However, MnTE treatment after IL-4 polarization had virtually no effect on

M2 markers. Thus, MnTE modulates short-term IL-4 signaling. It is unlikely that MnTE is modifying macrophage polarization by activating other transcription factors via increased ROS production. These data indicate that ROS is required during M2 polarization, likely as a ROS burst during the initial signaling events, and that MnTE is inhibiting M2 polarization and acting as an antioxidant in this specific context.

3.8. ROS is required for IL4-induced Stat3 activation.

We next examined key signaling pathways during M2 polarization to determine the MnTE-mediated mechanism of inhibition. Stat6 is a major transcription factor during M2 polarization and is activated via canonical type I IL-4 signaling [45]. Additionally, Stat6 has been shown be regulated by H_2O_2 during IL-4 signaling [46–48]. Although we found that MnTE inhibited IL4-mediated Stat6 activation in some cases, this effect is inconsistent amongst the various donor samples, suggesting that another pathway was involved in this phenomena (Supplemental Figure S2). Therefore, we next turned our attention toward the less studied type II IL-4 signaling, which activates Stat3 via dimerization of the IL-4Rα with the IL-13Rα1 receptor [49, 50]. Additionally, ROS is known to activate Stat3 [51, 52]. Stimulation of macrophages with IL-4 clearly increased Stat3 phosphorylation at Y705, indicating activation (Figure 8A–B). MnTE treatment resulted in a reduction of phospho-Stat3 levels in four human donors and in a dose dependent manner compared to the PBS controls (Figure 8A–B). Furthermore, DPI was used to determine if inhibiting Nox-derived ROS would also inhibit Stat3 activation, as it reduced M2 markers. Similar to MnTE, DPI treatment reduced phospho-Stat3 levels compared to DMSO control (Figure 8C). Furthermore, the M2 markers genes, IL-10, CD163, and PD-L2, are known target genes of Stat3 [53–55]. These M2 markers are all suppressed by drug treatment as indicated earlier in this study. All these studies clearly showed that either scavenging ROS with MnTE or inhibiting Nox activities with DPI, reduce phospho-Stat3 levels and inhibit Stat3 activation.

4. Discussion:

It is well known that cancer cells have higher intracellular ROS levels than their normal counterparts. It is also becoming clear that the tumor microenvironment (TME) is highly oxidized compared to their normal tissue counterparts. However, the role of the oxidative TME on cellular functions within the tumor remains relatively understudied. It has been shown that the oxidative TME contributes to immunosuppression in cancer, where increased extracellular ROS inhibited CD8+ T cell activation while inducing Treg activation [56–60]. Our data show that M2 or TAM-like macrophages have increased redox buffer, suggesting their high tolerance within the oxidative TME. Additionally, this study indicates ROS is a necessary secondary messenger for proper M2 polarization and function. Furthermore, addition of exogenous hydrogen peroxide promotes M2 polarization. Thus, it is reasonable to speculate that the oxidative TME may actively promote an immunosuppressive environment via polarizing TAM to a M2-like phenotype, while also inhibiting T cell activation and increasing Tregs.

Due to the plasticity of macrophages, there are a plethora of studies examining the differences in M1 and M2 states via large scale transcriptomics. Some key differences in

the expression levels of ROS producing and scavenging enzymes was identified by Beyer *et al* in M1 vs. M2 macrophages [61]. Their results show that M2 macrophages have increased expression of genes in the peroxiredoxin family, specifically PRDX1, PRDX3, and PRDX6, which may further contribute to the lower levels of ROS in M2 macrophages. Some of the largest changes in ROS-related genes were seen in the glutathione-S-transferase (GST) family, specifically lower GSTO1 and higher GSTP1, mGST2, and GSTT1, in M2 macrophages, which may lead to different glutathionylation patterns as a potential regulator of macrophage polarization and function. Our data agree with their RNA-seq data that Nox2 is the highest expressed Nox family member with the others being very lowly expressed or undetectable. Their observations also support our findings of differential expression of Nox2, Duox1, DuoxA1, MnSOD, catalase, Gpx1, and Cu/ZnSOD in M1 and M2 macrophages. Our study also takes these data a step further by analyzing the protein and activity levels of these genes, as well as analyze the effect of these changes on the redox status of M1 and M2 macrophages.

Our data implicate ROS as a required secondary messenger during IL-4 signaling for optimal M2 polarization. Furthermore, our data shows optimal M2 polarization, in part, requires Stat3 activation. The ability of ROS to promote Stat3 activation has been shown in other cell types [51, 62–66]. Additionally, hydrogen peroxide has been demonstrated to activate Jak2 and Tyk2, which are upstream activators of Stat3 [62, 66, 67]. Our studies imply that this ROS is likely generated from Nox2, as it is the most abundant ROS producing enzyme in these macrophages. Further supporting this, the pan-Nox inhibitor, DPI suppressed Stat3 activation and reduced M2 marker expression. However, DPI is a flavoprotein inhibitor that can inhibit enzymes other than Noxs, such as nitric oxide synthases, xanthine oxidases, and enzymes involved in the pentose phosphate pathway and TCA cycle [68]. Therefore, we cannot rule out the possibility that DPI may also inhibit M2 polarization through modulation of metabolic pathways [69]. Due to the use of primary human macrophages, the ability to genetic silence Nox member to test this hypothesis was limited. However, a study using mouse macrophages derived from the Nox1/2 double knockout mice noticed a similar M2 polarization deficiency [70]. Although it was unclear whether this deficiency occurred during macrophage differentiation or during M2 polarization, this study supports our speculation that Nox-generated ROS contributes to M2 macrophage polarization and their pro-tumorigenic phenotype.

ROS typically act as a secondary messenger during signaling through reversible oxidation and inactivation of protein tyrosine phosphatases (PTPs), which are the off switches of many signaling pathways. Therefore, we hypothesize that Nox2-derived ROS oxidizes and inactivates PTPs that are negatively regulating the IL-4 signaling pathway. Among the long list of PTPs that have been shown to negatively regulate Stat3 are SHP-1, SHP-2, PTP1B, and TCPTP, all of which can be inhibited via ROS-mediated reversible oxidation [71–74]. Furthermore, this mechanism may also be applicable to additional pathways that activate Stat3. These include IL-6, IL-10, and IL-22, which polarize macrophages to similar states as the IL-4 stimulated M2 used in this study [75–77]. Additionally, non-macrophage cells in the TME, such as myeloid-derived suppressor cells, are known to require Stat3 activation and ROS production for their immunosuppressive phenotype [60, 78]. Thus, MnTE may

have a wider ability to inhibit Stat3-mediated immunosuppression in macrophages and MDSCs than what our study examined.

Additional research indicates that MnTE also acts on other immune cells besides macrophages. In $CD4^+$ T cells, it skews their polarization by promoting T_H1 response and inhibiting T_H2 *in vivo* [79, 80]. Interestingly, Stat3 is required for optimal T_H2 polarization and function [81]. Due to closely related process of macrophage and $CD4^+$ T cell polarization, we speculate that MnTE inhibits M2 polarization and T_H2 polarization via similar mechanisms [2]. Furthermore, MnTE increases both $CD4^+$ and $CD8^+$ T cells in the spleen, as well as B cells and NK cells, suggesting it is activating several different types of immune cells that may provide additional anti-tumor effects [82]. It also increased production of IL-2, an immunostimulatory cytokine released primarily via T_H1 $CD4^+$ T cells. Additionally, tumor mouse models treated with MnTE or its analog, MnTnBuOE-2-PyP^{5+} affect monocyte infiltration and have increased M1 macrophages [83]. Our study adds evidence that MnTE also stimulates the immune system through inhibiting M2 polarization.

Several strategies have been proposed to target TAM for antitumor therapy. These include blocking macrophage recruitment to the tumor, decreasing total macrophage number via targeting therapies, and reprogramming of TAMs from the pro-tumorigenic M2 to proinflammatory M1 macrophages [84]. Reprogramming TAM has shown efficacy as a single therapy in inhibiting tumor growth and metastasis, thereby promoting survival in mouse models [85, 86]. While MnTE does not entirely reverse the M2 markers, this study clearly shows that it inhibits some of the critical negative effects of M2 macrophages. Additionally, the immunosuppressive function of TAM is a known mechanism of resistance to immune checkpoint blockade inhibitors [87]. Therefore, use of MnTE, to reprogram immunosuppressive TAM in combination with inhibitors for immune checkpoint blockade to stimulate T cell activation, presents a potentially promising and exciting combination approach to overcome this known resistance mechanism to immunotherapy.

5. Conclusion:

In conclusion, this study further confirms key differences between M1 and M2 macrophages in their production and scavenging of superoxide and hydrogen peroxide hinted at in previous studies. Additionally, we show that clinically relevant redox-active drugs could be used as a promising approach to selectively target M2 macrophages to inhibit their pro-tumorigenic and immunosuppressive functions. This study also supports the concept of the oxidative TME in actively and purposefully promoting M2 polarization in TAM. Future studies are required to determine the direct role of the oxidative TME on cell-cell interactions within the tumor. Additionally, more studies are need to determine the efficacy of MnTE to inhibit M2 polarization in tumor models *in vivo*, as well as in combination with T cell activating immunotherapy to synergistically reduce tumor growth.

Supplementary Material

Refer to Web version on PubMed Central for supplementary material.

Acknowledgements:

This work was financially supported by grants from the NIH R0I-CA182086A (Teoh-Fitzgerald), Redox Biology Pilot Project Fund (NTSBRDF, Uni. of Nebraska, Lincoln) (Teoh-Fitzgerald), and COBRE Nebraska Center for Cellular Signaling Collaborative Pilot Project grant (P30 GM106397). Brandon Griess was supported by the Eppley Institute in Cancer Biology Training Grant (NCI T32CA009476). EPR spectroscopy data were collected in the University of Nebraska EPR Spectroscopy Core, which is supported in part, by the National Institute of General Medical Sciences of the National Institute of Health (P30GM103335) awarded to the University of Nebraska's Redox Biology Center.

Abbreviations:

MnTE	MnTE-2-PyP^{5+}
MnP	Manganese Porphyrin
SOD	superoxide dismutase
c.m.	conditioned media
DHE	dihydroethidium
DCFH	2', 7'-dichlorodihydrofluorescein diacetate
HBSS	Hank's balanced salt solution
Gpx	glutathione peroxidase
Nox	NADPH oxidase
ROS	reactive oxygen species
TAM	tumor associated macrophage
BHA	butylated hydroxyanisole
Stat	signal transducer and activator of transcription
TME	tumor microenvironment
GST	glutathione S-transferases
MDSC	myeloid derived suppressor cells
PBMC	peripheral blood mononuclear cell
PTP	protein tyrosine phosphatase
GSH	glutathione
GSSG	oxidized glutathione
DPI	diphenyleneiodonium

References

1. Murray Peter J., et al. , Macrophage Activation and Polarization: Nomenclature and Experimental Guidelines. Immunity, 2014. 41(1): p. 14–20. [PubMed: 25035950]
2. Martinez FO and Gordon S, The M1 and M2 paradigm of macrophage activation: time for reassessment. F1000prime reports, 2014. 6: p. 13–13. [PubMed: 24669294]
3. Leek RD, et al. , Association of Macrophage Infiltration with Angiogenesis and Prognosis in Invasive Breast Carcinoma. Cancer Research, 1996. 56(20): p. 4625–4629. [PubMed: 8840975]
4. Mantovani A, et al. , Tumour-associated macrophages as treatment targets in oncology. Nature Reviews Clinical Oncology, 2017. 14: p. 399.
5. Bingle L, Brown NJ, and Lewis CE, The role of tumour-associated macrophages in tumour progression: implications for new anticancer therapies. J Pathol, 2002. 196(3): p. 254–65. [PubMed: 11857487]
6. Baghdadi M, et al. , High co-expression of IL-34 and M-CSF correlates with tumor progression and poor survival in lung cancers. Sci Rep, 2018. 8(1): p. 418. [PubMed: 29323162]
7. Ni Chao, Y. L, Xu Qiuran, Yuan Hongjun, Wang Wei, Xia Wenjie, Gong Dihe, Zhang Wei, Yu Kun, CD68- and CD163-positive tumor infiltrating macrophages in non-metastatic breast cancer: a retrospective study and meta-analysis. Journal of Cancer, 2019. 10(19): p. 4463–4472. [PubMed: 31528210]
8. Chen X, et al. , Prognostic value of diametrically polarized tumor-associated macrophages in multiple myeloma. Oncotarget, 2017. 8(68): p. 112685–112696. [PubMed: 29348856]
9. Jensen TO, et al. , Macrophage markers in serum and tumor have prognostic impact in American Joint Committee on Cancer stage I/II melanoma. J Clin Oncol, 2009. 27(20): p. 3330–7. [PubMed: 19528371]
10. Klein JL, et al. , CD163 immunohistochemistry is superior to CD68 in predicting outcome in classical Hodgkin lymphoma. Am J Clin Pathol, 2014. 141(3): p. 381–7. [PubMed: 24515766]
11. Komohara Y, et al. , Macrophage infiltration and its prognostic relevance in clear cell renal cell carcinoma. Cancer Sci, 2011. 102(7): p. 1424–31. [PubMed: 21453387]
12. Kridel R, et al. , The Prognostic Impact of CD163-Positive Macrophages in Follicular Lymphoma: A Study from the BC Cancer Agency and the Lymphoma Study Association. Clin Cancer Res, 2015. 21(15): p. 3428–35. [PubMed: 25869385]
13. Lee CH, et al. , Prognostic significance of macrophage infiltration in leiomyosarcomas. Clin Cancer Res, 2008. 14(5): p. 1423–30. [PubMed: 18316565]
14. Maniecki MB, et al. , Tumor-promoting macrophages induce the expression of the macrophage-specific receptor CD163 in malignant cells. Int J Cancer, 2012. 131(10): p. 2320–31. [PubMed: 22362417]
15. Yu M, et al. , Prognostic value of tumor-associated macrophages in pancreatic cancer: a meta-analysis. Cancer Manag Res, 2019. 11: p. 4041–4058. [PubMed: 31118813]
16. Biswas SK and Mantovani A, Macrophage plasticity and interaction with lymphocyte subsets: cancer as a paradigm. Nature Immunology, 2010. 11: p. 889. [PubMed: 20856220]
17. Ivan S, et al. , Breast cancer expression of CD163, a macrophage scavenger receptor, is related to early distant recurrence and reduced patient survival. International Journal of Cancer, 2008. 123(4): p. 780–786. [PubMed: 18506688]
18. Klingen TA, et al. , Tumor-associated macrophages are strongly related to vascular invasion, non-luminal subtypes, and interval breast cancer. Human Pathology, 2017. 69: p. 72–80. [PubMed: 28923419]
19. Medrek C, et al. , The presence of tumor associated macrophages in tumor stroma as a prognostic marker for breast cancer patients. BMC Cancer, 2012. 12(1): p. 306. [PubMed: 22824040]
20. Satu T, et al. , High numbers of macrophages, especially M2-like (CD163-positive), correlate with hyaluronan accumulation and poor outcome in breast cancer. Histopathology, 2015. 66(6): p. 873–883. [PubMed: 25387851]
21. Fritz JM, et al. , Depletion of Tumor-Associated Macrophages Slows the Growth of Chemically Induced Mouse Lung Adenocarcinomas. Frontiers in Immunology, 2014. 5(587).

22. Galmbacher K, et al. Shigella mediated depletion of macrophages in a murine breast cancer model is associated with tumor regression. PloS one, 2010. 5, e9572 DOI: 10.1371/journal.pone.0009572. [PubMed: 20221397]
23. Rogers TL and Holen I, Tumour macrophages as potential targets of bisphosphonates. Journal of Translational Medicine, 2011. 9(1): p. 177. [PubMed: 22005011]
24. Tan HY, et al. , The Reactive Oxygen Species in Macrophage Polarization: Reflecting Its Dual Role in Progression and Treatment of Human Diseases. Oxid Med Cell Longev, 2016. 2016: p. 2795090. [PubMed: 27143992]
25. Murata Y, Shimamura T, and Hamuro J, The polarization of T(h)1/T(h)2 balance is dependent on the intracellular thiol redox status of macrophages due to the distinctive cytokine production. Int Immunol, 2002. 14(2): p. 201–12. [PubMed: 11809739]
26. Zhang Y, et al. , ROS play a critical role in the differentiation of alternatively activated macrophages and the occurrence of tumor-associated macrophages. Cell Res, 2013. 23(7): p. 898–914. [PubMed: 23752925]
27. Festjens N, et al. , Butylated hydroxyanisole is more than a reactive oxygen species scavenger. Cell Death Differ, 2006. 13(1): p. 166–9. [PubMed: 16138110]
28. Gad SC, et al. , A Nonclinical Safety Assessment of MnTE-2-PyP, a Manganese Porphyrin. International Journal of Toxicology, 2013. 32(4): p. 274–287. [PubMed: 23704100]
29. Batinic-Haberle I, Tovmasyan A, and Spasojevic I, Mn Porphyrin-Based Redox-Active Drugs: Differential Effects as Cancer Therapeutics and Protectors of Normal Tissue Against Oxidative Injury. Antioxid Redox Signal, 2018. 29(16): p. 1691–1724. [PubMed: 29926755]
30. Tong Q, et al. , MnTE-2-PyP reduces prostate cancer growth and metastasis by suppressing p300 activity and p300/HIF-1/CREB binding to the promoter region of the PAI-1 gene. Free Radical Biology and Medicine, 2016. 94: p. 185–194. [PubMed: 26944191]
31. Tong Q, et al. , MnTE-2-PyP modulates thiol oxidation in a hydrogen peroxide-mediated manner in a human prostate cancer cell. Free Radical Biology and Medicine, 2016. 101: p. 32–43. [PubMed: 27671770]
32. Tovmasyan A, et al. , Radiation-Mediated Tumor Growth Inhibition Is Significantly Enhanced with Redox-Active Compounds That Cycle with Ascorbate. Antioxid Redox Signal, 2018. 29(13): p. 1196–1214. [PubMed: 29390861]
33. Rabbani ZN, et al. , Antiangiogenic action of redox-modulating Mn(III) meso-tetrakis(N-ethylpyridinium-2-yl)porphyrin, MnTE-2-PyP(5+), via suppression of oxidative stress in a mouse model of breast tumor. Free Radic Biol Med, 2009. 47(7): p. 992–1004. [PubMed: 19591920]
34. Policastro LL, et al. , The Tumor Microenvironment: Characterization, Redox Considerations, and Novel Approaches for Reactive Oxygen Species-Targeted Gene Therapy. Antioxid Redox Signal, 2012.
35. Cross AR and Jones OTG, The effect of the inhibitor diphenylene iodonium on the superoxide-generating system of neutrophils. Specific labelling of a component polypeptide of the oxidase. Biochemical Journal, 1986. 237(1): p. 111–116. [PubMed: 3800872]
36. Mia S, et al. , An optimized protocol for human M2 macrophages using M-CSF and IL-4/IL-10/TGF-β yields a dominant immunosuppressive phenotype. Scandinavian journal of immunology, 2014. 79(5): p. 305–314. [PubMed: 24521472]
37. Teoh MLT, et al. , Modulation of Reactive Oxygen Species in Pancreatic Cancer. Clinical Cancer Research, 2007. 13(24): p. 7441–7450. [PubMed: 18094428]
38. Teoh MLT, et al. , Overexpression of Extracellular Superoxide Dismutase Attenuates Heparanase Expression and Inhibits Breast Carcinoma Cell Growth and Invasion. Cancer Research, 2009. 69(15): p. 6355–6363. [PubMed: 19602586]
39. Weydert CJ and Cullen JJ, MEASUREMENT OF SUPEROXIDE DISMUTASE, CATALASE, AND GLUTATHIONE PEROXIDASE IN CULTURED CELLS AND TISSUE. Nature protocols, 2010. 5(1): p. 51–66. [PubMed: 20057381]
40. Yeung OWH, et al. , Alternatively activated (M2) macrophages promote tumour growth and invasiveness in hepatocellular carcinoma. Journal of Hepatology, 2015. 62(3): p. 607–616. [PubMed: 25450711]

41. Yuan A, et al. , Opposite Effects of M1 and M2 Macrophage Subtypes on Lung Cancer Progression. Scientific Reports, 2015. 5: p. 14273. [PubMed: 26399191]
42. Parsa R, et al. , Adoptive Transfer of Immunomodulatory M2 Macrophages Prevents Type 1 Diabetes in NOD Mice. Diabetes, 2012. 61(11): p. 2881–2892. [PubMed: 22745325]
43. Sharma A, et al., 77 - Immunotherapy of Cancer, in Clinical Immunology (Fifth Edition), Rich RR, et al., Editors. 2019, Content Repository Only!: London. p. 1033–1048.e1.
44. Huber S, et al. , Alternatively activated macrophages inhibit T-cell proliferation by Stat6-dependent expression of PD-L2. Blood, 2010. 116(17): p. 3311–3320. [PubMed: 20625006]
45. Lawrence T and Natoli G, Transcriptional regulation of macrophage polarization: enabling diversity with identity. Nat Rev Immunol, 2011. 11(11): p. 750–61. [PubMed: 22025054]
46. Dwivedi G, et al. , Dynamic Redox Regulation of IL-4 Signaling. PLOS Computational Biology, 2015. 11(11): p. e1004582. [PubMed: 26562652]
47. Kim HJ, et al. , Exogenous Hydrogen Peroxide Induces Lipid Raft-Mediated STAT-6 Activation in T Cells. Cellular Physiology and Biochemistry, 2017. 42(6): p. 2467–2480. [PubMed: 28848115]
48. Hirakawa S, et al. , Dual Oxidase 1 Induced by Th2 Cytokines Promotes STAT6 Phosphorylation via Oxidative Inactivation of Protein Tyrosine Phosphatase 1B in Human Epidermal Keratinocytes. The Journal of Immunology, 2011. 186(8): p. 4762–4770. [PubMed: 21411736]
49. Wills-Karp M and Finkelman FD, Untangling the Complex Web of IL-4- and IL-13-Mediated Signaling Pathways. Science Signaling, 2008. 1(51): p. pe55–pe55. [PubMed: 19109238]
50. Rahaman SO, Vogelbaum MA, and Haque SJ, Aberrant Stat3 Signaling by Interleukin-4 in Malignant Glioma Cells: Involvement of IL-13Rα2. Cancer Research, 2005. 65(7): p. 2956–2963. [PubMed: 15805299]
51. Liu J, et al. , The ROS-mediated activation of IL-6/STAT3 signaling pathway is involved in the 27-hydroxycholesterol-induced cellular senescence in nerve cells. Toxicology in Vitro, 2017. 45: p. 10–18. [PubMed: 28739487]
52. Choi SY, et al. , Reactive oxygen species mediate Jak2/Stat3 activation and IL-8 expression in pulmonary epithelial cells stimulated with lipid-associated membrane proteins from Mycoplasma pneumoniae. Inflammation Research, 2012. 61(5): p. 493–501. [PubMed: 22270622]
53. Cheng Z, et al. , CD163 as a novel target gene of STAT3 is a potential therapeutic target for gastric cancer. Oncotarget, 2017. 8(50): p. 87244–87262. [PubMed: 29152078]
54. Hedrich CM, et al. , Stat3 promotes IL-10 expression in lupus T cells through trans-activation and chromatin remodeling. Proceedings of the National Academy of Sciences, 2014. 111(37): p. 13457–13462.
55. Garcia-Diaz A, et al. , Interferon Receptor Signaling Pathways Regulating PD-L1 and PD-L2 Expression. Cell Reports, 2017. 19(6): p. 1189–1201. [PubMed: 28494868]
56. Chen X, et al. , Reactive Oxygen Species Regulate T Cell Immune Response in the Tumor Microenvironment. Oxidative Medicine and Cellular Longevity, 2016. 2016: p. 1580967. [PubMed: 27547291]
57. Kraaij MD, et al. , Induction of regulatory T cells by macrophages is dependent on production of reactive oxygen species. Proc Natl Acad Sci U S A, 2010. 107(41): p. 17686–91. [PubMed: 20861446]
58. Sklavos MM, Tse HM, and Piganelli JD, Redox modulation inhibits CD8 T cell effector function. Free Radical Biology and Medicine, 2008. 45(10): p. 1477–1486. [PubMed: 18805480]
59. Kraaij MD, et al. , Dexamethasone increases ROS production and T cell suppressive capacity by anti-inflammatory macrophages. Molecular Immunology, 2011. 49(3): p. 549–557. [PubMed: 22047959]
60. Nagaraj S, et al. , Altered recognition of antigen is a mechanism of CD8+ T cell tolerance in cancer. Nature Medicine, 2007. 13: p. 828.
61. Beyer M, et al. , High-resolution transcriptome of human macrophages. PLoS One, 2012. 7(9): p. e45466. [PubMed: 23029029]
62. Simon AR, et al. , Activation of the JAK-STAT pathway by reactive oxygen species. American Journal of Physiology-Cell Physiology, 1998. 275(6): p. C1640–C1652.

63. Yu MO, et al. , Reactive oxygen species production has a critical role in hypoxia-induced Stat3 activation and angiogenesis in human glioblastoma. Journal of Neuro-Oncology, 2015. 125(1): p. 55–63. [PubMed: 26297045]
64. Millonig G, et al. , Sustained Submicromolar H2O2 Levels Induce Hepcidin via Signal Transducer and Activator of Transcription 3 (STAT3). Journal of Biological Chemistry, 2012. 287(44): p. 37472–37482. [PubMed: 22932892]
65. Carballo M, et al. , Oxidative Stress Triggers STAT3 Tyrosine Phosphorylation and Nuclear Translocation in Human Lymphocytes. Journal of Biological Chemistry, 1999. 274(25): p. 17580–17586. [PubMed: 10364193]
66. Ju KD, et al. , Potential role of NADPH oxidase-mediated activation of Jak2/Stat3 and mitogen-activated protein kinases and expression of TGF-β1 in the pathophysiology of acute pancreatitis. Inflammation Research, 2011. 60(8): p. 791–800. [PubMed: 21509626]
67. Tawfik A, et al. , Hyperglycemia and reactive oxygen species mediate apoptosis in aortic endothelial cells through Janus kinase 2. Vascular Pharmacology, 2005. 43(5): p. 320–326. [PubMed: 16257269]
68. Riganti C, et al. , Diphenyleneiodonium inhibits the cell redox metabolism and induces oxidative stress. J Biol Chem, 2004. 279(46): p. 47726–31. [PubMed: 15358777]
69. Galván-Peña S and O'Neill LAJ, Metabolic reprograming in macrophage polarization. Frontiers in immunology, 2014. 5: p. 420–420. [PubMed: 25228902]
70. Xu Q, et al. , NADPH Oxidases Are Essential for Macrophage Differentiation. J Biol Chem, 2016. 291(38): p. 20030–41. [PubMed: 27489105]
71. Xu D and Qu C-K, Protein tyrosine phosphatases in the JAK/STAT pathway. Frontiers in bioscience : a journal and virtual library, 2008. 13: p. 4925–4932. [PubMed: 18508557]
72. Persson C, et al. , Preferential oxidation of the second phosphatase domain of receptor-like PTP-alpha revealed by an antibody against oxidized protein tyrosine phosphatases. Proceedings of the National Academy of Sciences of the United States of America, 2004. 101(7): p. 1886–1891. [PubMed: 14762163]
73. Gross S, et al. , Inactivation of protein-tyrosine phosphatases as mechanism of UV-induced signal transduction. J Biol Chem, 1999. 274(37): p. 26378–86. [PubMed: 10473595]
74. Meng T-C, et al. , Regulation of Insulin Signaling through Reversible Oxidation of the Protein-tyrosine Phosphatases TC45 and PTP1B. Journal of Biological Chemistry, 2004. 279(36): p. 37716–37725. [PubMed: 15192089]
75. Luo Wei, Y. B, Qin Qin-Yi, Lu Jiong-Min, Qin Shan-Yu, Jiang Hai-Xing, Interleukin-22 promotes macrophage M2 polarization via STAT3 pathway. International Journal of Clinical and Experimental Medicine, 2016. 9(10): p. 19574–19580.
76. Fu X-L, et al. , Interleukin 6 induces M2 macrophage differentiation by STAT3 activation that correlates with gastric cancer progression. Cancer Immunology, Immunotherapy, 2017. 66(12): p. 1597–1608. [PubMed: 28828629]
77. Niemand C, et al. , Activation of STAT3 by IL-6 and IL-10 in primary human macrophages is differentially modulated by suppressor of cytokine signaling 3. J Immunol, 2003. 170(6): p. 3263–72. [PubMed: 12626585]
78. Vasquez-Dunddel D, et al. , STAT3 regulates arginase-I in myeloid-derived suppressor cells from cancer patients. J Clin Invest, 2013. 123(4): p. 1580–9. [PubMed: 23454751]
79. Jungsuwadee P, et al. , The Metalloporphyrin Antioxidant, MnTE-2-PyP, Inhibits Th2 Cell Immune Responses in an Asthma Model. International Journal of Molecular Sciences, 2012. 13(8): p. 9785–9797. [PubMed: 22949830]
80. Snelgrove RJ, et al. , In the Absence of Reactive Oxygen Species, T Cells Default to a Th1 Phenotype and Mediate Protection against Pulmonary Cryptococcus neoformans Infection. The Journal of Immunology, 2006. 177(8): p. 5509–5516. [PubMed: 17015737]
81. Stritesky GL, et al. , The Transcription Factor STAT3 Is Required for T Helper 2 Cell Development. Immunity, 2011. 34(1): p. 39–49. [PubMed: 21215659]
82. MAKINDE AY, et al. , Effect of a Metalloporphyrin Antioxidant (MnTE-2-PyP) on the Response of a Mouse Prostate Cancer Model to Radiation. Anticancer Research, 2009. 29(1): p. 107–118. [PubMed: 19331139]

83. Ashcraft KA, et al. , Novel Manganese-Porphyrin Superoxide Dismutase-Mimetic Widens the Therapeutic Margin in a Preclinical Head and Neck Cancer Model. Int J Radiat Oncol Biol Phys, 2015. 93(4): p. 892–900. [PubMed: 26530759]

84. Sawa-Wejksza K and Kandefer-Szerszeń M, Tumor-Associated Macrophages as Target for Antitumor Therapy. Archivum Immunologiae et Therapiae Experimentalis, 2018. 66(2): p. 97–111. [PubMed: 28660349]

85. Coscia M, et al. , Zoledronic acid repolarizes tumour-associated macrophages and inhibits mammary carcinogenesis by targeting the mevalonate pathway. J Cell Mol Med, 2010. 14(12): p. 2803–15. [PubMed: 19818098]

86. Georgoudaki A-M, et al. , Reprogramming Tumor-Associated Macrophages by Antibody Targeting Inhibits Cancer Progression and Metastasis. Cell Reports, 2016. 15(9): p. 2000–2011. [PubMed: 27210762]

87. Cassetta L and Kitamura T, Targeting Tumor-Associated Macrophages as a Potential Strategy to Enhance the Response to Immune Checkpoint Inhibitors. Frontiers in Cell and Developmental Biology, 2018. 6: p. 38. [PubMed: 29670880]

Highlights:

- M1 and M2 macrophages have distinct ROS profiles.
- M2 macrophages require ROS during IL-4 stimulated polarization.
- MnTE-2-PyP, a SOD mimetic, selectively inhibits M2 polarization and function.

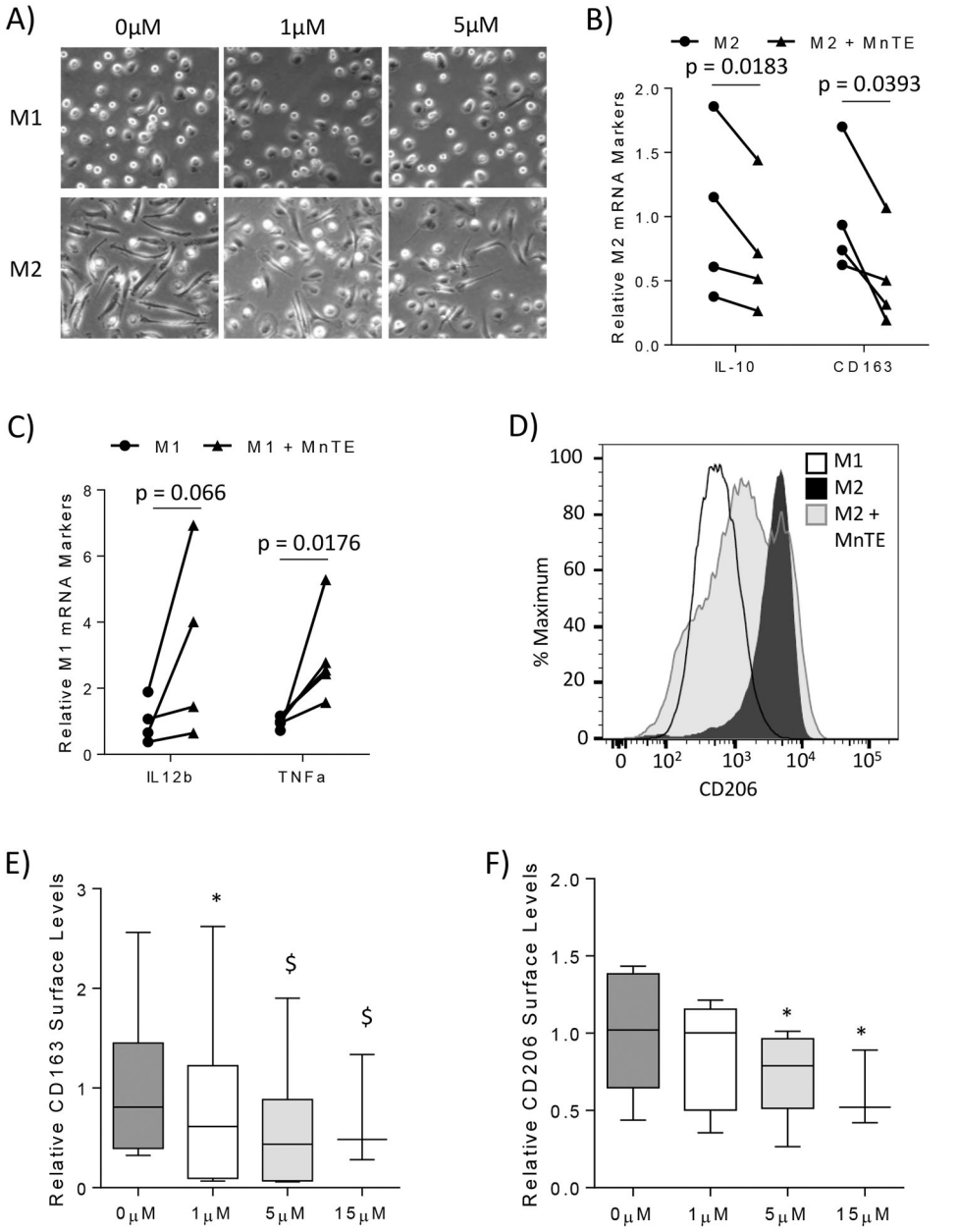

Figure 1).

MnTE inhibits M2 polarization. Primary human macrophages were generated from isolated monocytes which were differentiated to macrophages and polarized to M1 or M2 types. The macrophages were analyzed 24 hours after polarization. (A) Representative phase contrast pictures of M1 and M2 macrophages treated with varying concentrations of MnTE. Expression of (B) M1 and (C) M2 mRNA markers in macrophages treated with or without 15 μM MnTE from 3 and 4 different donors, respectively. (D) A representative histogram of CD206 surface staining in M1 and M2 macrophages. (E, F) A box plot graph depicting flow cytometry analysis of M2 surface marker levels in M2 macrophages from 6 different donors treated with varying concentrations of MnTE. Relative values were calculated by comparing the change of MnTE treated samples to its untreated donor-specific control. Student t-test

was used to calculate p-value for figures 1B and 1C. A one-way ANOVA followed by a post-hoc Tukey test was used to determine significance of samples treated with different concentrations of MnTE in figures 1E and 1F. Symbols indicate significance between the treatment groups and M2 control (* < 0.05, $ < 0.005, # < 0.0005).

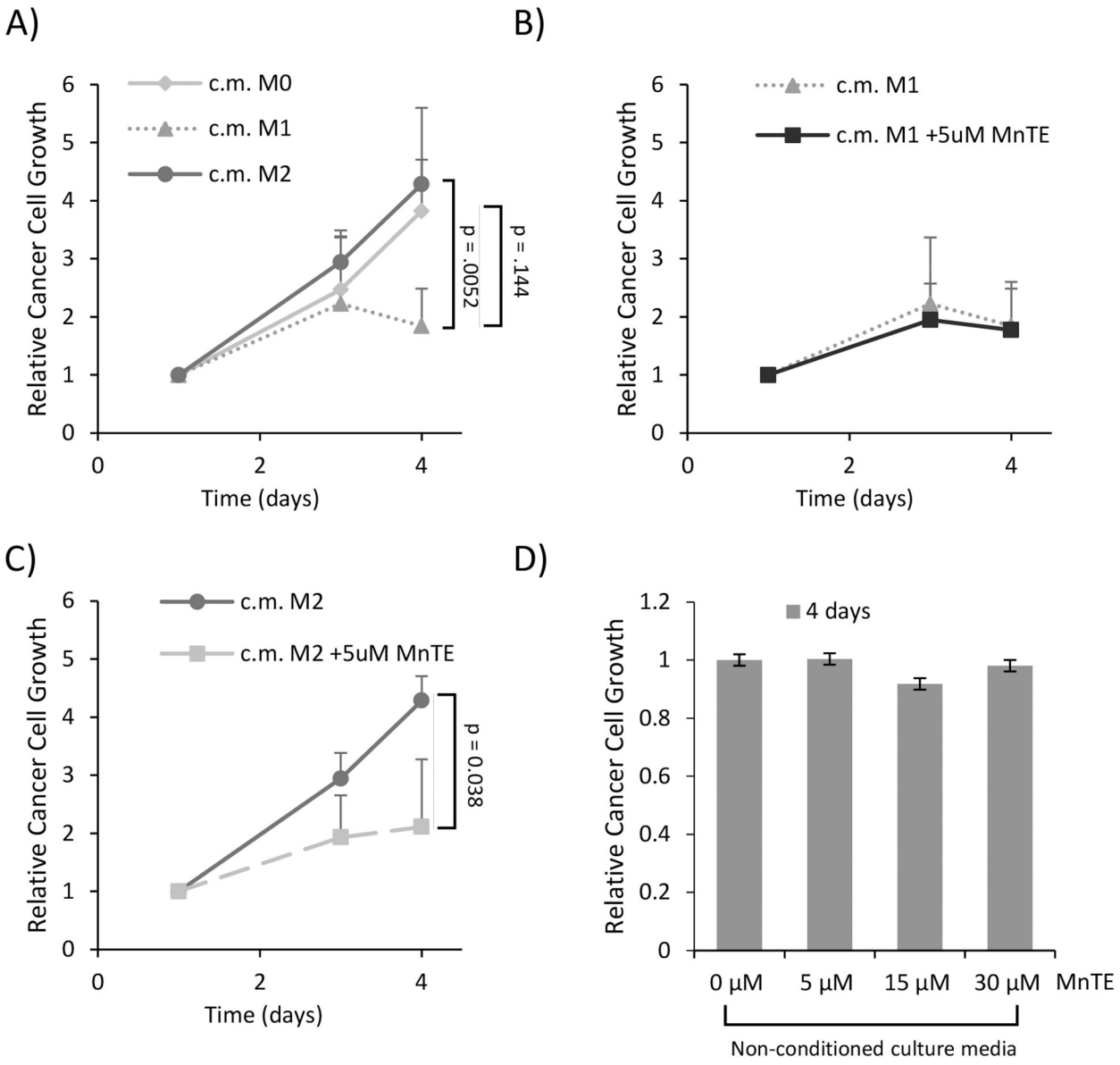

Figure 2).

MnTE treatment inhibits M2-mediated cancer cell growth. MDA-MB231 breast cancer cells were grown in 50% conditioned media from M1 or M2 macrophages, with or without MnTE pre-treatment. (A-C) Line graphs depicting the relative growth of MDA-MB231 cancer cells in macrophage conditioned media from 4 different donors. (A) This line graph compares growth of MDA-MB231 in the control conditioned media (of unstimulated M0 macrophages) to M1 and M2 macrophages. (B-C). Line graphs depicting the effect of 5 µM MnTE pre-treatment on (B) M1 and (C) M2 macrophage conditioned media versus control conditioned media. (D) The relative cancer cell growth after 4 days in unconditioned media with the addition of varying MnTE doses. Error bars are the standard deviation. Student t-test was used to calculate p-value with statistical significance being < 0.05. P-values between MnTE pretreated conditioned media and their respective controls are indicated by lines between the different groups.

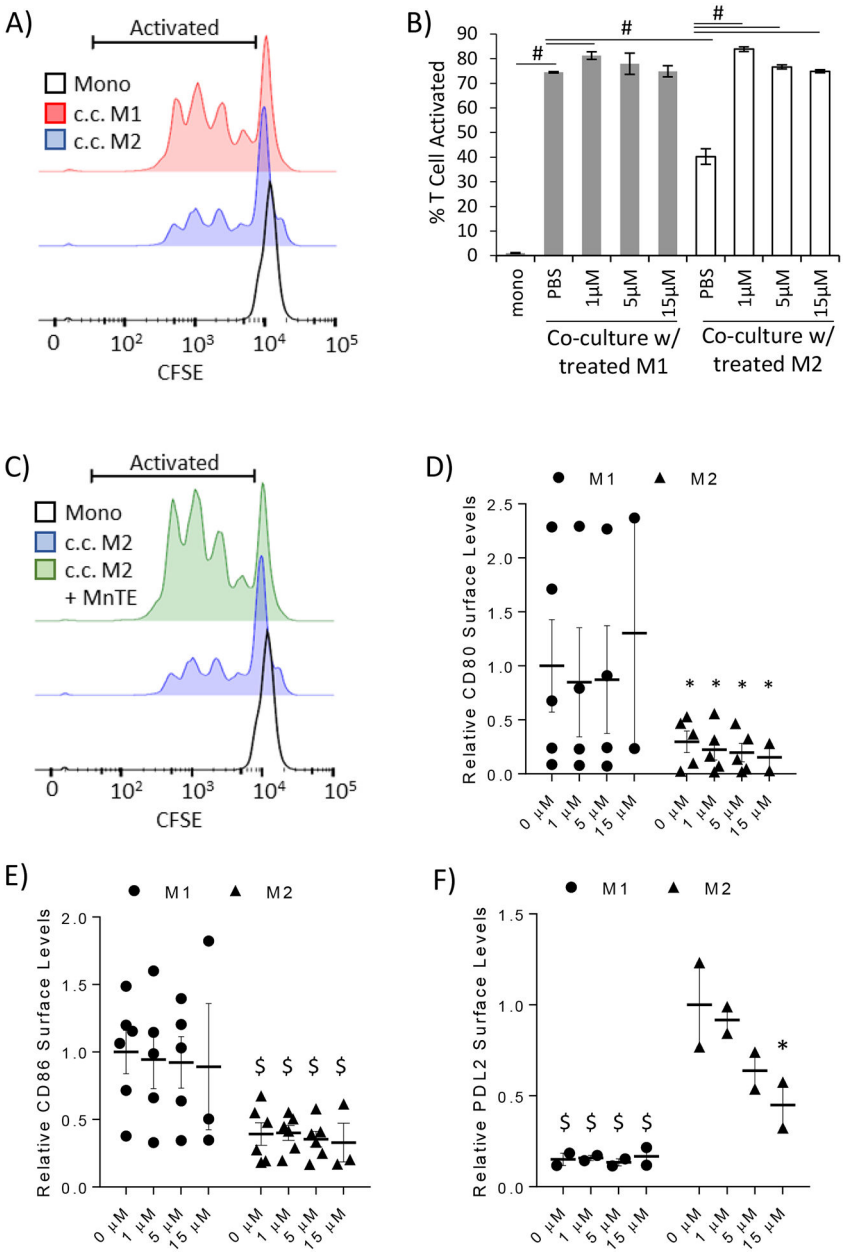

Figure 3).

MnTE inhibits M2-mediated T cell suppression. A T cell activation assay was performed to assess the ability of macrophages to modify T cell activation. Human peripheral blood lymphocytes (PBLs) were stained with CFSE to track their activation. PBLs were directly co-cultured with autologous control of pre-treated macrophages and stimulated with anti-CD3. Flow cytometry was used to track the dilution of CFSE as a proxy for T cell activation. (A) A representative histogram of T cells comparing unstimulated mono-culture T cells with anti-CD3 stimulated T cells co-cultured with either M1 or M2 macrophages. The bracket delineates the activated T cells measured in the bar graph. (B) A bar graph depicting the average percent T cell activated after direct co-culture with the control or pre-treated M1 and M2 macrophages. Four technical replicates from a representative donor are shown

here. Similar results were obtained in 3 different donors. (C) A representative histogram highlighting the ability of pre-treated M2 macrophages to promote T cell activation. (D-F) Flow cytometry analysis of surface markers known to affect T cell activation in treated M1 and M2 macrophages. The following co-activators of (D) CD80, (E) CD86 were analyzed. Relative expression levels of the co-inhibitory molecule, PD-L2 is shown in (F). A two-way ANOVA followed by post-hoc Tukey test was used to calculate p-value with statistical significance being < 0.05. Symbols indicate significance between the M1 control group and the indicated sample in figures 1D–E. The symbols in figure 1F indicate statistical significance between the M2 control group and the indicated sample (* < 0.05, $ < 0.005, # < 0.0005).

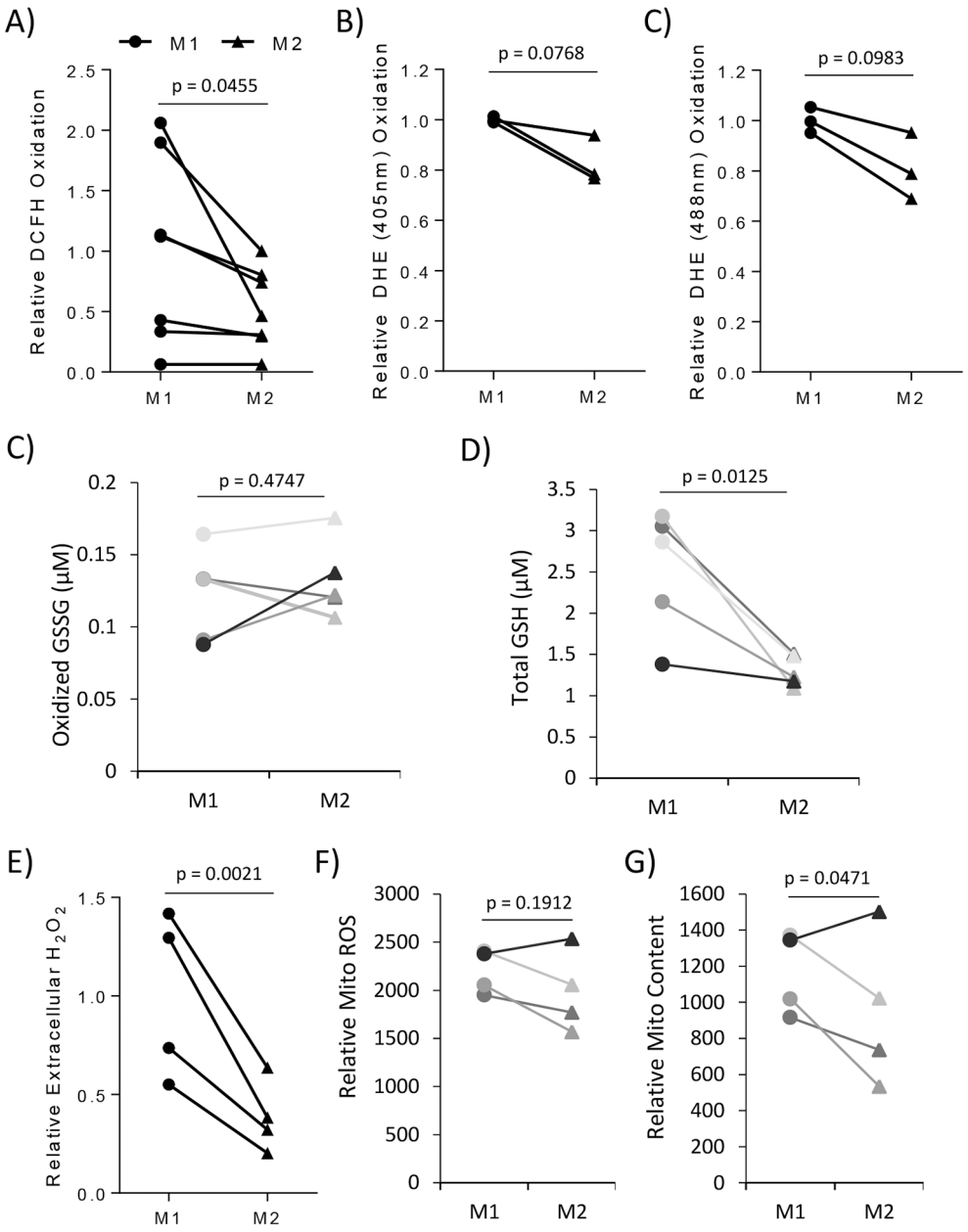

Figure 4).

M2 macrophages have differential redox status compared to M1. Primary human macrophages were analyzed after 24 hours of polarization. The ROS levels of primary human macrophages from 7 different human donors were measured by (A) DCFH. (B) DHE measured ROS levels in primary human macrophages from 4 different donors. DHE excitation at 405nm and 488nm was used to measure superoxide-specific levels and general ROS levels respectively. (C, D) The levels of oxidized GSSG and total GSH were measured using GSH/GSSG-glo assay in 5 different donors. (E) The levels of extracellular H_2O_2 were measured using AmplexRed via plate reader from 4 different donors. (F, G) The levels of mitochondrial ROS production and mitochondrial number in macrophages from 4 different donors were assessed using MitoSox and MitoTrackerGreen respectively.

Each color indicating changes between M1 and M2 for each specific donor. (A, B, F, G) Fluorescence was assessed using flow cytometry. Relative values were calculated by comparing the change of the M2 sample to its donor specific M1 sample making each change donor specific to account for the heterogeneity of different human donors. Error bars are the standard deviation between all donors M1 or M2 samples. Paired student t-test was used to calculate p-value with statistical significance being < 0.05.

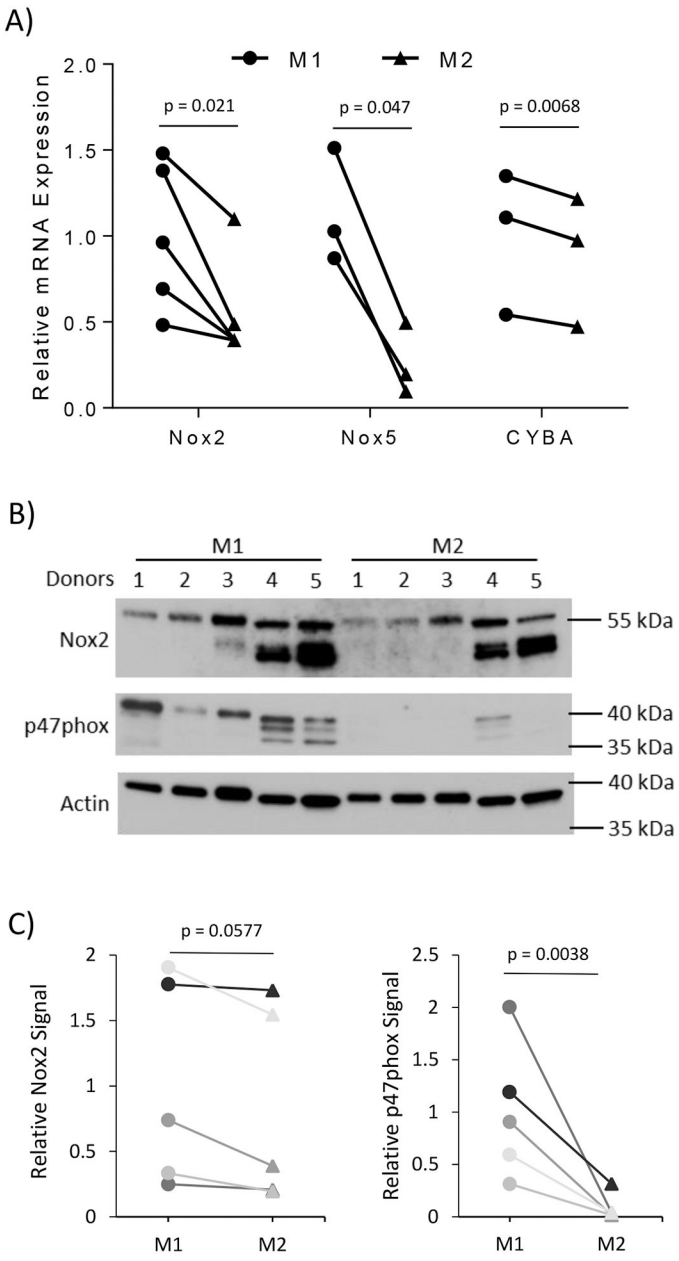

Figure 5).

M2 macrophages have lower ROS producers than M1. (A) Messenger RNA was isolated from M1 and M2 macrophages 24 hours after addition of polarizing cytokines. The mRNA expression of Nox family members and co-factors was measured using rt-qPCR. The differences between M1 and M2 were calculated using the ΔΔ Ct method with 18S as the loading control. Analysis of gene expression was performed using $N = 3–5$ donors. (B) The protein expression of Nox2, p47phox, and β-actin in M1 and M2 macrophages was analyzed using Western blot analysis from 5 different donors. (C) Densitometry analysis of Nox2 and p47phox compared to the loading control, β-actin, is indicated in line graphs comparing the change of the change of M2 sample to its donor specific M1 sample to account for the heterogeneity of different human donors. The bar graphs indicate the average

gene expression with error bars indicating the standard deviation. Paired student t-test was used to calculate p-value with statistical significance being < 0.05.

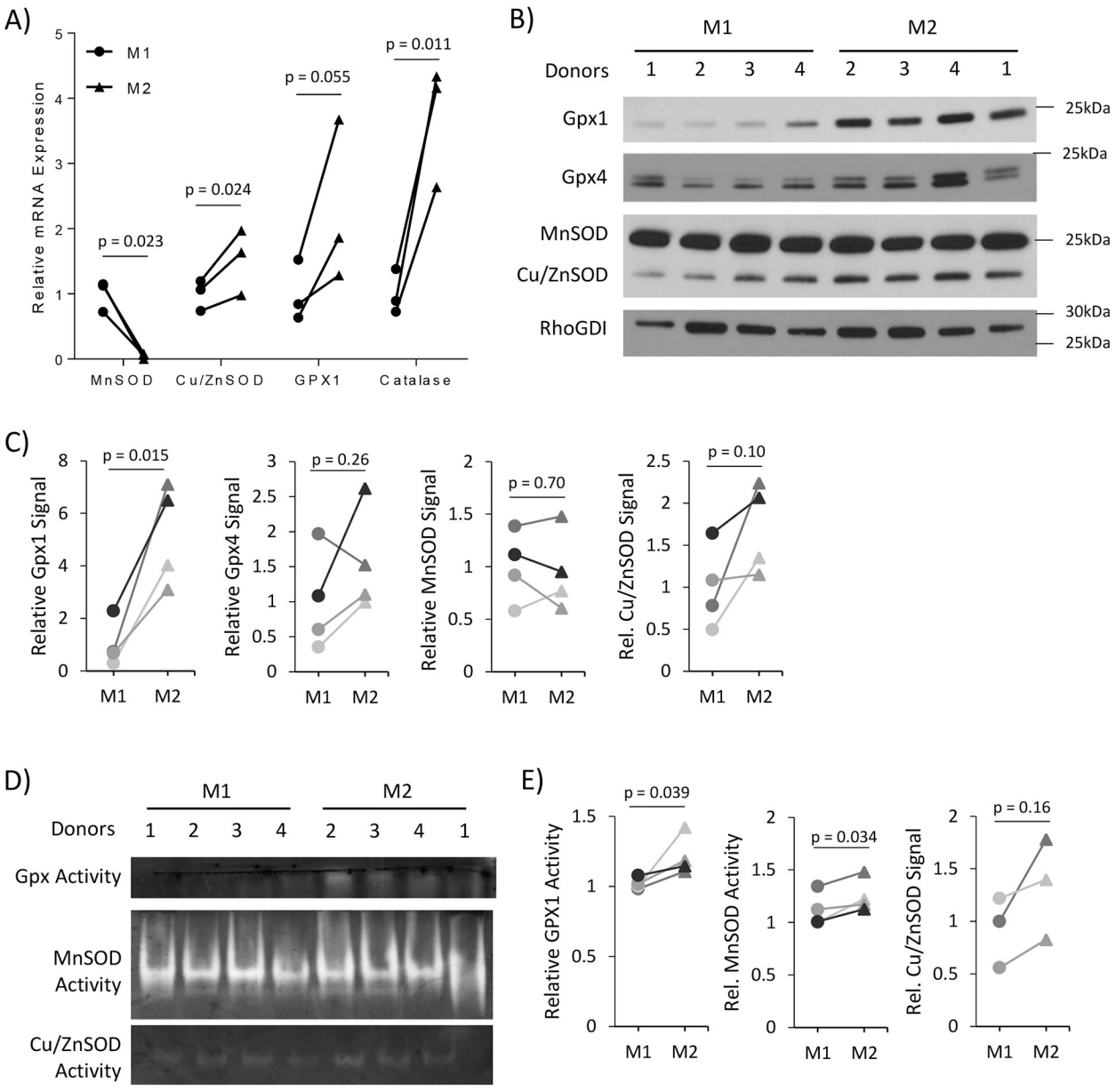

Figure 6).

M2 macrophage have higher antioxidant enzyme expression and activity compared to M1. (A) Antioxidant gene expression was measured using rt-qPCR to determine differences between M1 and M2 macrophages. Analysis of gene expression was performed using *N = 3–4* donors. (B) Western blot analysis of antioxidant genes indicating the differential protein levels between M1 and M2 macrophages from 4 different donors. (C) Densitometry analysis of Gpx1, Gpx4, MnSOD, and Cu/ZnSOD compared to the loading control, RhoGDI. The line graphs indicate the relative difference between M1 and M2 samples of each individual donor. (D) In-gel activity assays for Gpx and SOD proteins using M1 and M2 whole cell lysate. (E) Densitometry analysis of Gpx and SOD in-gel activity assays. Paired student t-test was used to calculate p-value with statistical significance being < 0.05.

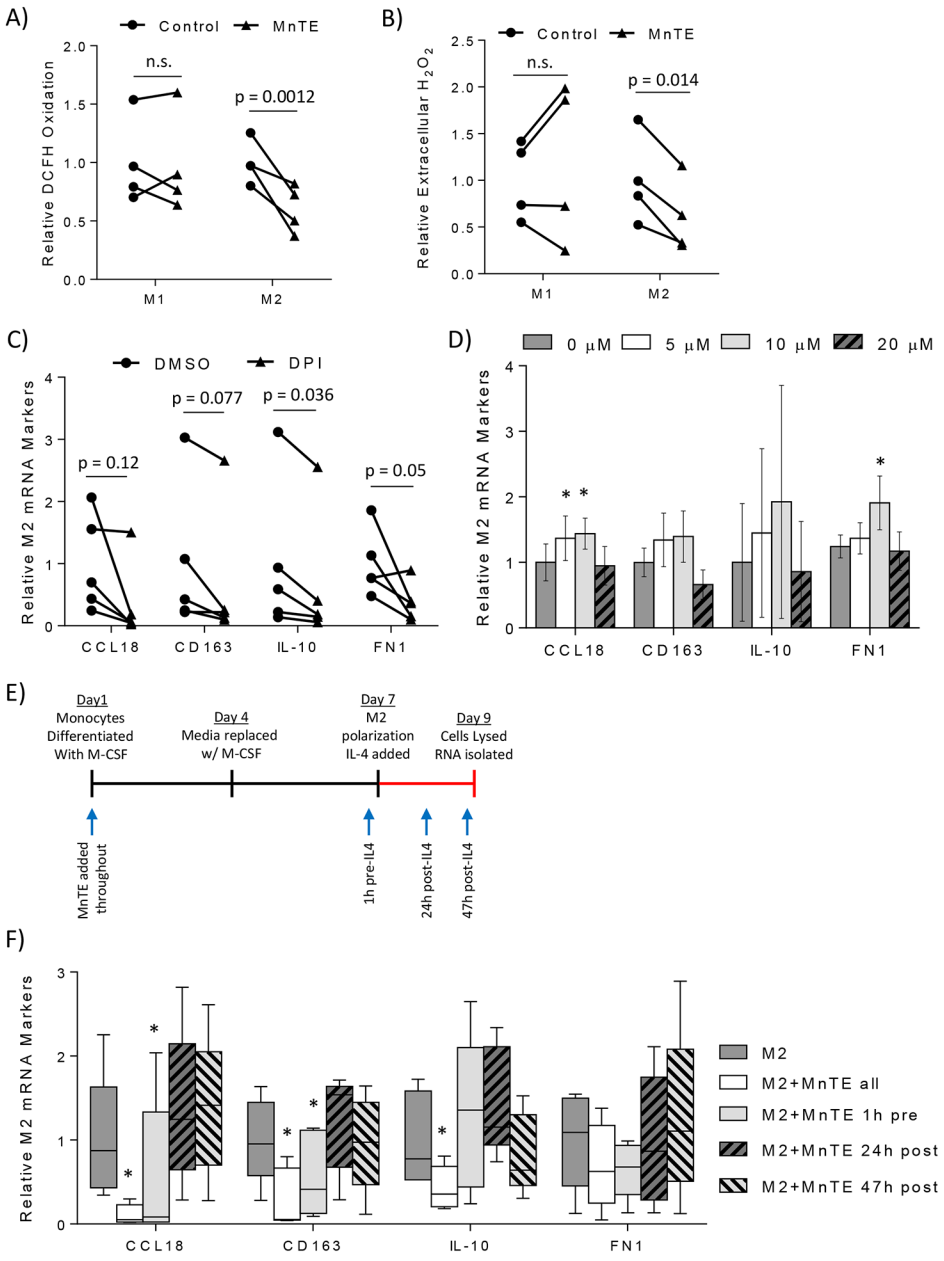

Figure 7).

ROS is a required secondary messenger during IL-4 stimulated M2 polarization. (A) Flow cytometry analysis of ROS levels using DCFH in M1 and M2 macrophages from 4 different donors treated with or without 15 μM MnTE. (B) Bar graph depicting the relative change in extracellular H_2O_2 levels in control versus 15 μM MnTE treated M1 and M2 macrophages from 4 different donors. (C, D) Measurement of M2 mRNA markers 24 hours after addition of IL-4. Macrophages were treated with either (C) DMSO or 10 μM DPI for 1 hour before addition of IL-4 or (D) exogenous H_2O_2 immediately after addition of IL-4. (E, F) Macrophages were treated with MnTE at different times throughout the differentiation and polarization protocol. (E) Diagram indicating the M2 polarization protocol with arrows indicating when MnTE was added in the different samples. (F) Relative M2 mRNA marker

expression of macrophages compared to untreated control measured 48 hours after addition of IL-4. Error bars are the standard error of the mean. A paired student t-test was used to calculate the displayed p-values for figures 7A, 7B, and 7C. A one-way ANOVA and a post-hoc Tukey test was performed for figures 7D and 7F. Symbols indicate significance between the M2 control group and the indicated treatment group (* < 0.05, $ < 0.005, # < 0.0005).

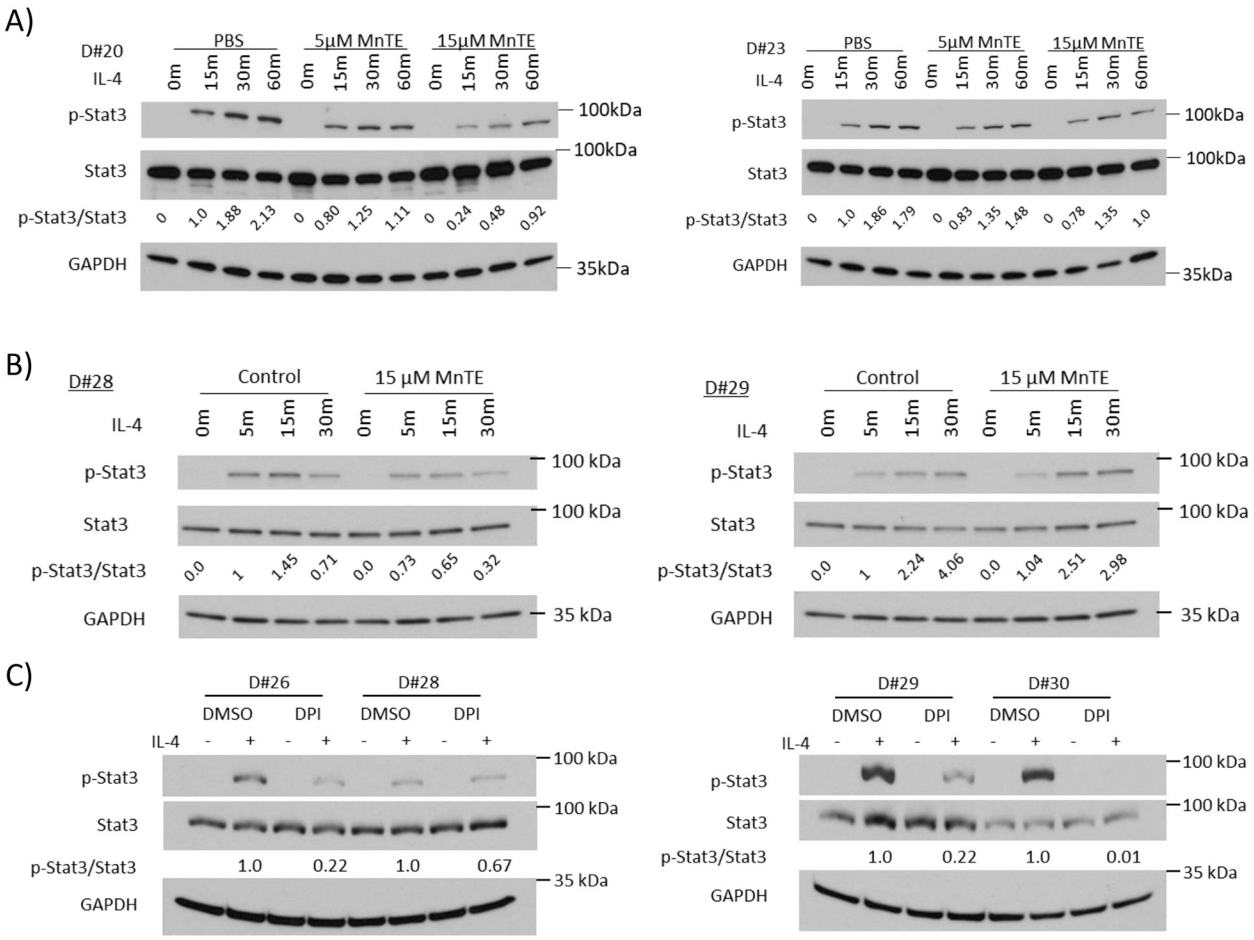

Figure 8).

MnTE inhibits Stat3 activation. (A-C) Western blot analysis of p-Stat3, total Stat3, and loading control GAPDH in macrophages from different donors treated with MnTE or DPI. Macrophages were serum starved overnight before IL-4 addition. Macrophages were stimulated with IL-4 for varying time points indicated above each lane. The densitometry indicating the relative p-Stat3/total Stat3 ratio is include below the total Stat3 blot. (A) Macrophages were treated with PBS or MnTE (5 μM or 15 μM) throughout differentiation and IL-4 stimulation. (B) Macrophages were treated with PBS or MnTE (15 μM) 1 hour before addition of IL-4. (C) Macrophages were treated with DMSO or DPI (10 μM) for 1 hour before stimulation with IL-4.